Role of fines on cohesive behavior of mine tailings inferred from critical shear stress

Africa M. Geremew and Ernest K. Yanful

Abstract: The significance of fines on the cohesive behavior of mine tailings has been investigated by examining the incipient motion of the tailings. Sixteen laboratory experiments were performed in a Plexiglas laboratory annular column on reconstituted mine tailings under a 50 cm water cover. Re-suspension was produced by a Teflon stirrer and the velocity field in the column was characterized using a laser Doppler velocimeter (LDV). The pressure change in the boundary layer was also measured with a Preston tube. It was observed that the nondimensional critical shear stresses showed deviation from those of the noncohesive model results at a fines content greater than 50%–55%. An empirical relation that shows the relation between the boundary shear stress deviation and the percent fines in the tailings was proposed. Regression analysis of the experimental results showed that a power law relationship could reasonably be used to describe the relation between the measured nondimensional excess bed shear stress and the erosion rate. It is proposed that the value of β (the erosion rate constant) could be taken as 1 for mine tailings that show cohesive behavior.

Key words: mine tailings, critical shear stress, fines content, erosion rate, Preston tube.

Résumé : L'importance des particules fines dans le comportement en cohésion des rejets miniers a été étudiée par l'évaluation de l'amorce de mouvement des rejets. Seize essais en laboratoire ont été réalisés dans une colonne annulaire de Plexiglas sur des rejets miniers reconstitués et placés sous un recouvrement d'eau de 50 cm. La resuspension a été produite par un agitateur de Teflon et le champ des vitesses a été caractérisé par la vélocimétrie par laser Doppler (LDV). Les changements de pression dans la couche frontière ont aussi été mesurés à l'aide d'un tube Preston. Il a été observé que les contraintes critiques de cisaillement non dimensionnelles démontrent une déviation par rapport à celles obtenues par un modèle non cohésif lorsque le contenu en particules fines était supérieur à 50–55 %. Une relation empirique, qui exprime le lien entre la déviation de la contrainte de cisaillement à la frontière et le pourcentage de particules fines dans les rejets, est proposée. Une analyse de régression des résultats expérimentaux a démontré qu'une loi de puissance peut être utilisée de façon raisonnable afin de décrire la relation entre la contrainte de cisaillement excessive non dimensionnelle du lit et le taux d'érosion. Il est proposé que la valeur de β (la constante du taux d'érosion) puisse être égale à 1 pour les rejets miniers qui présentent un comportement cohésif.

Mots-clés : rejets miniers, contrainte critique de cisaillement, contenu en particules fines, taux d'érosion, tube Preston.

[Traduit par la Rédaction]

Introduction

The use of a shallow water cover over mine waste is one of the most effective techniques for managing acid-generating tailings because tailings oxidation is dramatically reduced due to the lower diffusivity and solubility of oxygen in water than in air. However, erosion and subsequent re-suspension of tailings by environmental loadings (loads from wind-induced water waves and pressure-driven countercurrent flows) may lead to tailings oxidation and then to environmental pollution if the water cover depth is insufficient. As a result, sufficient water cover depth that does not allow or allows only permissible re-suspension needs to be provided. In the design of an optimum water cover for mine tailings, critical shear stress is one of the required basic parameters. The critical bed shear stress is usually estimated analytically for noncohesive sediments and experimentally for cohesive sediments. Therefore, understanding the cohesive nature of mine tailings is critical.

Natural sediments can be classified as noncohesive or cohesive. Noncohesive sediments have a granular structure and the individual sediment particles do not stick together. The erosion behavior of such sediments is influenced mainly by their particle size, solid density, and particle shape. Cohesive sediments contain significant amounts of clay-sized material, which have strong inter particle forces due to their surface ionic charges. As particle size decreases, surface area per unit volume (i.e., specific surface) increases, and interparticle forces (not the gravitational force) dominate the behavior of sediments. The erosion behavior of cohesive sediments is not influenced mainly by the particle size and density of individual particles. There is no clear boundary between cohesive and noncohesive sediments as far as surface erosion is concerned; their definition is usually site-specific. In general, finer-sized sediments (<2 μm) are considered cohesive and coarser-sized sediments (>63 μm) are considered noncohesive.

Received 10 April 2009. Accepted 30 September 2010. Published at www.nrcresearchpress.com/cgj on 12 April 2011.

A.M. Geremew and E.K. Yanful. Department of Civil and Environmental Engineering, The University of Western Ontario, 1151 Richmond Street North, London, ON N6A 5B9, Canada.

Corresponding author: A.M. Geremew (e-mail: ageremew@uwo.ca).

Fig. 1. Experimental (laboratory) annular column. All dimensions in centimetres.

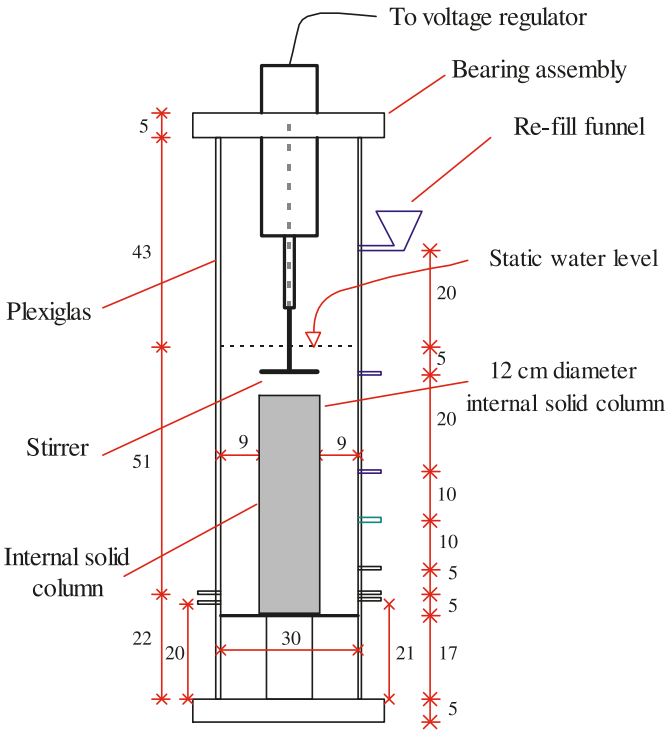

Intermediate silt-sized sediments (2–63 μm) are considered cohesive or noncohesive depending on other influencing factors.

A number of researchers have tried to establish criteria to distinguish between cohesive and noncohesive sediments. Soulsby (1997) reported that cohesion strongly influences the erosion process if the fines fraction of the sediment (<63 μm) is more than 10%. Mignoit (1981) considered cohesive sediments as those sediments that have a mean grain size less than 63 μm. The transition between cohesive and noncohesive sediments was suggested to be 3%–15% mud content (Mitchener and Torfs 1996; Whitehouse et al. 2000). Mitchell and Soga (1997) and others have defined cohesive sediments as those sediments that have clay content (<4 μm) above 5%–10%. McCave et al. (1995) proposed a 10 μm cut-off for sortability of sediments in their transport model. Van Ledden et al. (2004) have proposed a sand–silt–clay ternary diagram that classifies six categories of sediments. They used average clay content (<4 μm) of 7.5% (5%–10%) as a classifying criterion between cohesive and noncohesive sediments.

Surface erosion of cohesive sediments is influenced mainly by physical, electrochemical, and biological factors. The physical factors include clay content, water content, clay type, temperature, bulk density, and pore pressure (Raudkivi 1998), whereas the electrochemical factors include the chemistry of eroding and pore fluid (Winterwerp et al. 1990). The biological processes may decrease sediment erodibility (e.g., bioturbation, a reworking or packing of the sediment bed by organisms), increase sediment erodibility (i.e., bio-stabilization) or be neutral (i.e., no effect) (Paterson and Daborn 1991; Paterson 1997).

There is not much published work that addresses cohesiveness in subaqueous sulphide mine tailings. Indeed, from experimental investigation of fine mine tailings, a number of researchers (Yanful and Catalan 2002; Peacey and Yanful 2003) have found that the erosion equation for tailings resembles that of natural cohesive sediments even at a low clay content (<2 μm) in some cases. This leads to two fundamental questions. Do all mine tailings behave like cohesive natural sediments? Can the classifying criterion (cohesive and noncohesive) for natural sediments be used for tailings? Therefore, the main objective of the present study was to attempt to answer these questions and, via these answers, establish a classification criterion for mine tailings based on their fines contents.

Materials and methods

Samples

The tailings samples used in the present study were laboratory re-constituted sulphide-bearing tailings obtained from the Mattabi mine tailings pond located near Ignace, Ontario, Canada. Sulfide-bearing tailings were also obtained from the Shebandowan mine tailings pond located near Shebandowan Lake approximately 90 km west of Thunder Bay, Ontario, Canada. Kaolinite, a 1:1 layer clay mineral obtained from United Clay Inc., Georgia, USA, was also used in the study.

Physical, chemical, and mineralogical characteristics of the tailings

A series of laboratory tests were carried out using standard testing methods to obtain the basic physical properties of the tailings. The particle-size distributions of the dried tailings were measured using a standard sieve and hydrometer analysis. The specific gravity was also measured. The classification of the tailings was based on American Society for Testing and Materials (ASTM) standard D2487 (Braja 2002). The salinity and pH of the eroding and pore fluids were measured with conductivity and pH meters, respectively. Tailings mineralogy was characterized using the X-ray diffraction method.

Experimental column description

The erosion experiments were performed in a transparent cylindrical Plexiglas annular column with an internal diameter of 30 cm, a height of 1.25 m, and a thickness of 1 cm. The annular flow width of the column was 9 cm. A 3 cm thick polyvinyl chloride (PVC) plate was screwed to the bottom of the column with a connection gasket to ensure watertightness. A 1 cm thick circular plate, made of Plexiglas, with a radius of 30 cm was fixed at 21 cm above the bottom of the column. This intermediate circular plate was supported by wooden pillars well glued to the wall of the column to ensure watertightness. The column had nine 1 cm diameter openings on its wall. Four of the openings, which were located at 10, 20, 30, and 50 cm from the surface of the intermediate plate, were used as sampling ports. One of the openings, which was located at 75 cm from the surface of the intermediate plate, was used for re-filling of water to compensate for the volume of suspension (sample) taken for the measurement of suspended solids concentration. The other two that were located at 5 cm from the intermediate plate were for pressure measurements. The remaining two

Table 1. Sample identification description.

No.	Sample description	Sample identification
1	Re-constituted Mattabi tailings sample - 01	Sample - 01
2	Re-constituted Mattabi tailings sample - 02	Sample - 02
3	Re-constituted Mattabi tailings sample - 03	Sample - 03
4	Re-constituted Mattabi tailings sample - 04	Sample - 04
5	Re-constituted Mattabi tailings sample - 05	Sample - 05
6	Re-constituted Mattabi tailings sample - 06	Sample - 06
7	Re-constituted Mattabi tailings sample - 07	Sample - 07
8	Re-constituted Mattabi tailings sample - 08	Sample - 08
9	Re-constituted Mattabi tailings sample - 09	Sample - 09
10	Re-constituted Mattabi tailings sample - 10	Sample - 10
11	Re-constituted Mattabi tailings sample - 11	Sample - 11
12	Re-constituted Mattabi tailings sample - 12	Sample - 12
13	Re-constituted Mattabi tailings sample - 13	Sample - 13
14	Re-constituted Shebandowan west cell tailings sample	Sample - 14
15	Re-constituted Mattabi tailings and kaolinite sample - 01	Sample - 15
16	Re-constituted Mattabi tailings and kaolinite sample - 02	Sample - 16

Note: Samples were re-constituted by fractionation as in Table 2.

Fig. 2. Particle-size distribution.

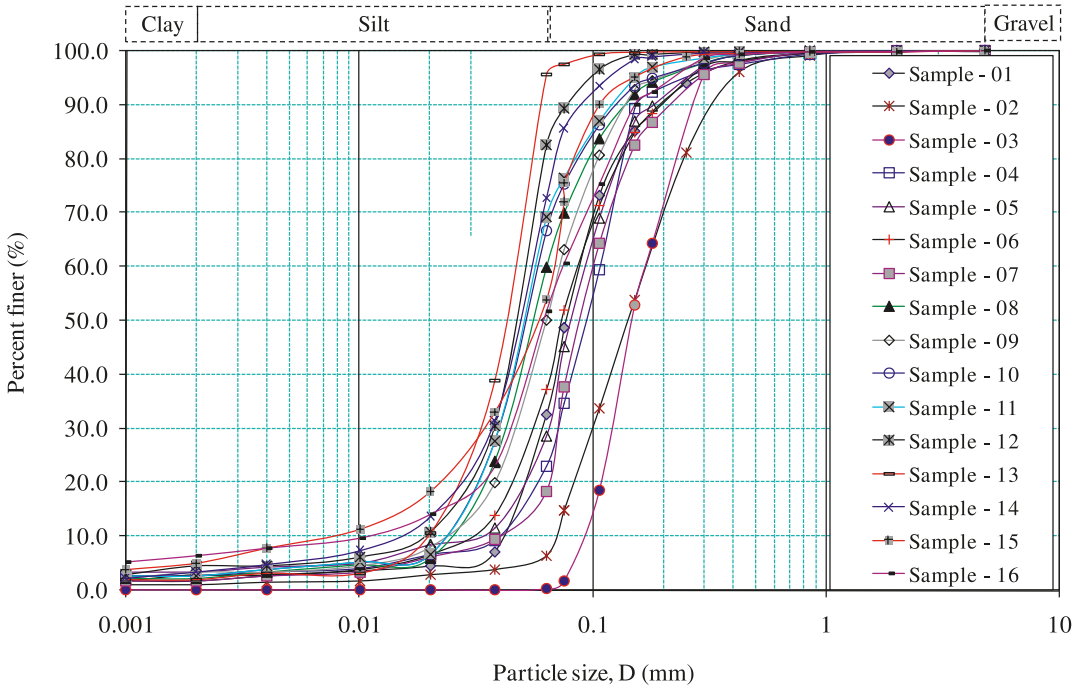

openings, located at 3 and 4 cm above the surface of the intermediate plate, were for pore-water pressure measurements. A 50 cm long two-blade Teflon stirrer was used to introduce bed shear stress. Each blade of the Teflon stirrer was 6 cm long and 1 cm thick. As shown in Fig. 1, the top 3 cm PVC cover plate was fitted with a bearing assembly to ensure that the stirrer was stationary. The stirrer was controlled by an alternating current (ac) motor and the input power to the stirrer was regulated by a direct current (dc) voltage regulator; the stirrer speed was calibrated against the voltage regulator with an accuracy of ±2%. As mentioned in the sample preparation section of this paper, a water cover of 50 cm, 5 cm thick tailings, and a consolidation time of 3 days were used in the column experiments.

Velocity measurements

The velocity field in the annular column was measured by laser Doppler velocimetry (LDV). The annular column was filled with water to obtain a water depth of 50 cm. Commercial seeding particles, titanium dioxide particles with size less than 2 μm, were introduced in the water to facilitate the measurement of instantaneous velocities. The water was stirred by a motor-driven Teflon stirrer. The speed of the motor ranged from 44 to 197 revolutions per minutes (rpm) and was increased in steps. For each stirrer speed, the vertical velocity profile at radial distances of 14, 11.5, 10, and 7 cm from the center of the column were measured with LDV. The LDV equipment used in this study was a Thermo Systems Inc (TSI) laser Doppler model LDP 100 (Thermo

Table 2. Physical and chemical properties of the re-constituted tailings samples of the present study.

	Physical properties					Chemical properties			
		Particle parameters				Salinity		pH	
Sample name	Specific gravity	D_{50} (mm)	ϕ_{clay} (%)	ϕ_{fine} (%)	ϕ_{sand} (%)	$S_{E\text{-}Fluid}$ (g/L)	$S_{P\text{-}Fluid}$ (g/L)	$P_{E\text{-}Fluid}$	$P_{P\text{-}Fluid}$
Sample - 01	2.93	0.077	1.75	32.66	67.34	0.148	0.214	4.75	3.23
Sample - 02	2.96	0.142	1.15	6.37	93.63	0.131	0.194	6.85	4.12
Sample - 03	2.93	0.146	0.00	0.26	99.74	0.135	0.159	6.85	4.25
Sample - 04	2.95	0.094	2.72	23.11	76.89	0.142	0.140	6.55	4.05
Sample - 05	3.09	0.081	3.46	28.60	71.40	0.130	0.123	6.60	4.15
Sample - 06	2.93	0.073	2.85	37.17	62.83	0.124	0.122	6.65	3.94
Sample - 07	2.99	0.089	1.87	18.23	81.77	0.122	0.086	6.45	4.49
Sample - 08	3.12	0.056	2.12	59.92	40.08	0.125	0.113	6.20	4.18
Sample - 09	3.07	0.063	3.39	50.06	49.94	0.121	0.098	6.35	4.27
Sample - 10	3.24	0.052	2.58	66.60	33.40	0.131	0.107	6.82	4.79
Sample - 11	3.29	0.051	2.60	69.21	30.79	0.126	0.149	6.50	4.15
Sample - 12	3.50	0.047	4.52	82.68	17.32	0.121	0.221	6.73	3.51
Sample - 13	3.63	0.043	2.02	95.71	4.29	0.245	0.093	6.92	4.55
Sample - 14	3.22	0.049	3.41	72.87	27.13	0.145	2.092	6.40	3.97
Sample - 15	3.07	0.058	5.14	53.95	46.05	0.212	0.136	7.67	6.76
Sample - 16	3.03	0.061	6.39	51.80	48.20	0.193	0.157	7.39	7.25

Note: D_{50}, average particle size diameter; ϕ_{clay}, percentage of clay (<2 μm); ϕ_{fine}, percentage of fines (<63 μm); ϕ_{sand}, percentage of sand; $S_{E\text{-}Fluid}$, salinity of eroding fluid; $S_{P\text{-}Fluid}$, salinity of pore fluid; $P_{E\text{-}Fluid}$, pH of eroding fluid; $P_{P\text{-}Fluid}$, pH of pore fluid.

Systems Inc., Shoreview, Minnesota, USA.). The laser Doppler probe was connected to a TSI Intelligent Flow Analyzer (IFA) 600 signal processor. The IFA signal processor was connected to a TSI model 6261 16-bit direct memory access (DMA) board and Laservec software.

Entrainment experiments

Sample preparation

The tailings were air-dried and sorted in size groups using standard sieves. Then, a series of samples were prepared by varying the clay-sized (<2 μm) fines and sand-sized tailings content. Each of the samples (Table 1) was prepared by mixing a pre-determined amount of tailings and regular tap water. The mixing was done manually with a wooden rod for about 20 min and a uniform suspension was produced. The whole suspension was immediately poured into the column and stirred again with the wooden rod for 5–10 min and then with a motor-driven stirrer for about 10 min. Finally, the suspension was allowed to settle and consolidate for 3 days, after which a bed layer, approximately 5 cm thick, was obtained. This process of sample preparation resembles natural settling and consolidation in natural lakes. In all the experiments, sample preparation was done to obtain an approximately 5 cm consolidated tailings layer and a 50 cm water cover. From each of the re-constituted samples in the laboratory, sufficient quantities were left for standard laboratory characterization.

The salinity of the tap water used was 0.115 g/L and its electrical conductivity was measured to be 253 $\mu s \cdot cm^{-1}$. The presence of chlorine (and other similar elements) in a treated tap water could decrease the biological oxidation rate while re-suspension using the Teflon stirrer could increase oxidation. Thus, eventually, the net effect of these two compensating factors on the critical shear stress would be negligible (Yanful and Verma 1999; Yanful et al. 2000; Mian and Yanful 2007).

For 13 of the samples that were re-constituted in the laboratory by air-drying the Mattabi tailings (samples 1–13), the parameters that could influence the surface erosion of the tailings, such as pH, sodium adsorption ratio, cation exchange capacity, salinity of the pore and eroding fluids, and mineralogy, were approximately the same. The same applied to the re-constituted tailings samples from Shebandowan west cell (sample 14) and Mattabi-Kaolinite mixes (samples 15 and 16). Moreover, the initial and boundary conditions including the consolidation time (i.e., 3 days for each sample) were the same. Therefore, in general, the main difference between the samples used in the study was the particle-size distribution (i.e., amount of clay, silt, fine and coarse sands).

Pore-water pressure measurement in the tailings

Once the tailings sample was deposited in the annular column and covered with 50 cm of water, it was left for consolidation for t3 days. During these 3 days of consolidation, the hydrostatic and total pore-water pressures at the mid-depth of the deposited tailings were measured with a pressure transducer. The hydrostatic pore-water pressure is the pore-water pressure at the steady-state condition, whereas the total pore-water pressure is the sum of hydrostatic and excess pore-water pressure. The opening at approximately mid-depth of the tailings in the column was connected to a pressure transducer (Model 245/345 Pressure Transmitter) which, in turn, was connected to a data logger – computer system.

Re-suspended solids measurement

The concentrations of re-suspended material were measured for 11 different rotational speeds of the stirrer, starting from 44 up to 197 rpm. Samples were obtained through the sampling ports 10, 20, 30, and 40 min after the stirrer speed

Table 3. Physical and chemical properties of different tailings.

	Physical properties					Chemical properties					
		Particle parameters				Salinity		pH			
Sample name	Specific gravity	D_{50} (mm)	ϕ_{clay} (%)	ϕ_{fine} (%)	$\phi_{f\text{-sand}}$ (%)	$S_{E\text{-Fluid}}$ (g/L)	$S_{P\text{-Fluid}}$ (g/L)	$P_{E\text{-Fluid}}$	$P_{P\text{-Fluid}}$	Experimental methods	References
Falconbridge NTA	3.80	0.040	23.00	73.00	27.00	~0.10–0.12[a]	—	~6.5–7.5[a]	~9–10	Rotating circular flume	Mian and Yanful (2007)
Premier Gold	3.60	0.010	7.00	97.00	3.00	~0.10–0.12[a]	—	~6.5–7.5[a]	—	Rotating circular flume	Samad and Yanful (2005)
Health Steele Upper Cell	3.80	0.012	10.00	95.00	5.00	~0.10–0.12[a]	—	~6.5–7.5[a]	~6.00	Rotating circular flume	Mian and Yanful (2007)
Coarse tailings	2.61	0.230	—	—	—	~0.10–0.12[a]	—	~6.5–7.5[a]	—	Wave flume	Davé et al. (2003)
Fine tailings	2.37	0.083	—	—	—	~0.10–0.12[a]	—	~6.5–7.5[a]	—	Wave flume	Davé et al. (2003)
Fine tailings covered with a 5 cm layer of fine silica sand	2.40	0.120	—	—	—	~0.10–0.12[a]	—	~6.5–7.5[a]	—	Wave flume	Davé et al. (2003)

Note: $\phi_{f\text{-sand}}$, percentage of fine sand; $S_{E\text{-Fluid}}$, salinity of eroding fluid; $S_{P\text{-Fluid}}$, salinity of pore fluid.
[a] Tap water.

was increased. Immediately after each sampling, an equivalent volume of water was supplied through the re-filling funnel (Fig. 1). The concentration of re-suspended solids for each stirrer speed was obtained by oven-drying the corresponding sampled suspension at 100 °C for approximately 24 h. By doing so, the concentration of re-suspended materials was related to the stirrer speed of the motor which, in turn, was related to the bed shear stress.

Results and discussion

Physical, chemical, biological, and mineralogical properties of the tailings

The particle-size distributions for the re-constituted tailings samples are shown in Fig. 2. Table 2 shows the key physical and chemical characteristics of the tailings. The Mattabi tailings were dark in colour, while Shebandowan west cell tailings were brown; both of them had no odor. As per the product specification, 95% of the kaolinite was finer than 2 μm.

An increase in electrolyte concentration of the pore water makes the diffuse double layer thinner. Thus, the interparticle repulsive force decreases and the erosion shear strength increases. A low pH solution of the pore fluid leads to positive edge to negative surface interaction leading to flocculation from suspension, whereas stable suspensions (dispersions) of clay particles often require a high pH value (Mitchell and Soga 1997). According to Partheniades (2006), a salinity value lower than 1 g/L has a negligible effect on both the viscosity and mechanical properties of suspended aggregates and deposited beds. The measured salinity of the pore and eroding fluid of the re-constituted samples of the Mattabi tailings (i.e., samples 1–13) was less than 0.214 g/L and the pH was between 3.23 and 6.85 (Table 2). These results suggest that the influence of salinity and pH on the critical shear stress of re-constituted Mattabi tailings was likely insignificant. The salinity and pH of the pore fluid of the Shebandowan tailings (sample 14) was 2.092 g/L and 3.97, respectively. The salinity of the eroding fluid was 0.145 g/L and its pH was 6.40. These results (for sample 14) suggest that salinity could play a significant role, say, by increasing critical shear stress. As shown in Table 2, the salinity of the pore and eroding fluids of the Mattabi tailings samples (samples 1–13) and the kaolinite–tailings mixed samples (samples 15 and 16) are well below 0.25 g/L and the pH values are between 3.5 and 7.3. These results suggest that salinity and pH would likely not significantly influence the critical shear stress for Mattabi tailings and kaolinite mixed tailings samples. Table 3 also shows the physical and chemical properties of different tailings used in erosion experiments in the rotating circular flume (RCF) and wave flume (WF).

Young and Southard (1978) observed that the critical shear stress values estimated from laboratory tests were larger than those estimated from the corresponding in situ values. They concluded that the difference in this critical shear stress was due to natural bioturbation. In the present study, the tailings were re-constituted in the laboratory under different particle-size distributions and the erosion experiments were conducted after only 3 days of consolidation. Hence, the biological influence on the initiation of motion and subsequent re-suspension of the tailings was probably insignificant and not accounted for in the analysis.

Fig. 3. X-ray powder pattern of Mattabi tailings.

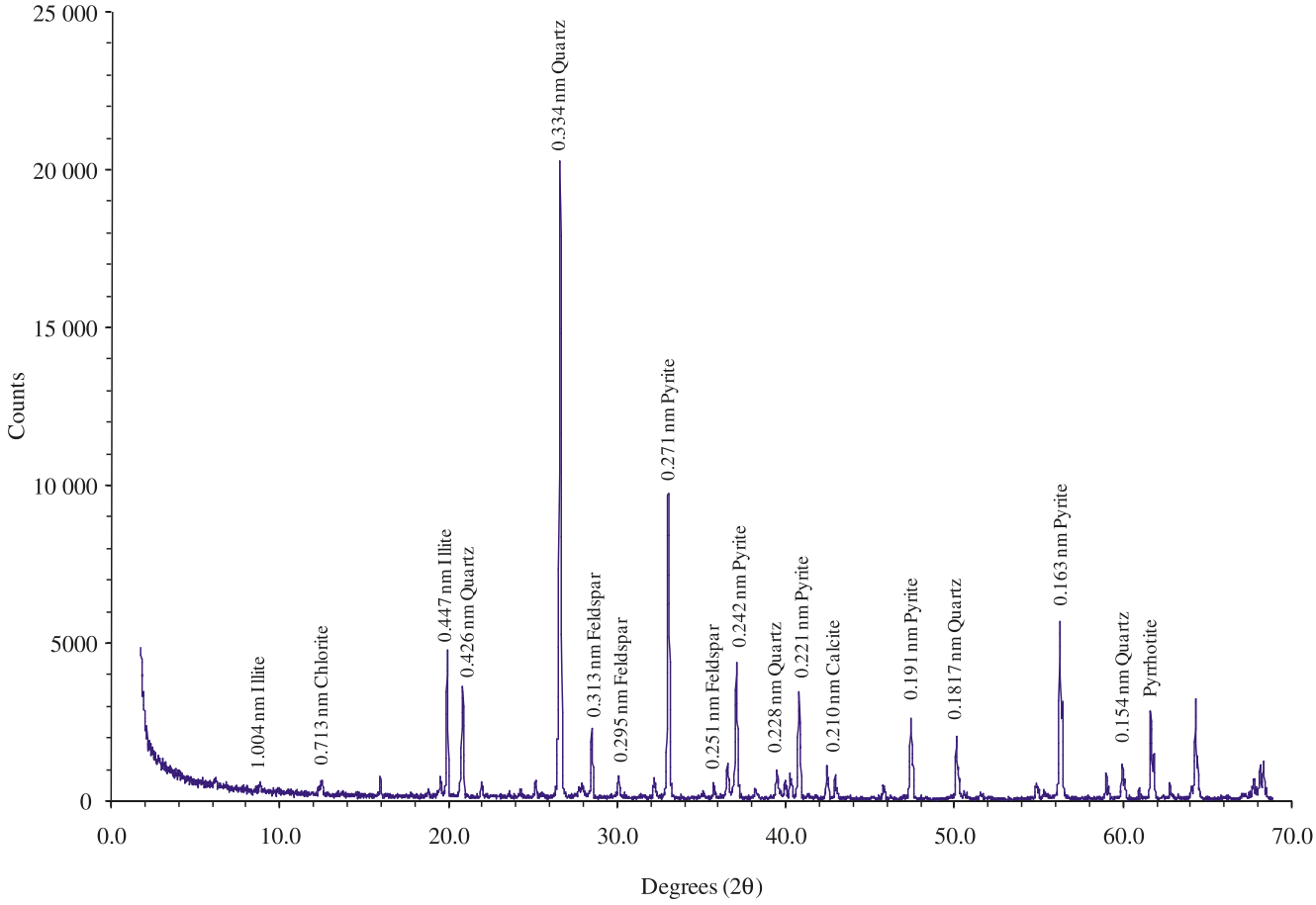

The results of the X-ray diffraction analysis indicate that the main components of the Mattabi tailings were illite, chlorite, feldspar, quartz, pyrite, and pyrrhotite (Fig. 3). The major minerals present in the Shebandowan tailings were kaolinite, chlorite, quartz, feldspar, pyrite, and pyrrhotite (Fig. 4). According to the product data provided by United Clay Inc., the kaolinite contained SiO_2 (45.7%), Al_2O_3 (37.4%), Fe_2O_3 (0.80%), Na_2O (0.05%), and K_2O (0.33%) and had a specific surface of 24.25 m^2/g.

Bed shear stress estimation

The flow-induced bed shear stress was estimated using two methods; namely, from the velocity profile and pressure change in the near-bed flow region (i.e., boundary layer). The water in the annular column was stirred with the motor-driven stirrer at a speed ranging from 44 to 197 rpm. For each stirrer speed, the velocity profile at radial distances of 14, 11, 10, and 7 cm from the center of the column were measured with LDV. The flow-induced bed shear stress was estimated from the near-bed velocity distribution. As per the previous work of Geremew and Yanful (2011) on the same annular column, the results of the near-bed velocity profiles followed a logarithmic law over the bottom wall. The relationship between the average bed shear stress and the stirrer speed was established and is given by eq. [1]

$$[1] \qquad \tau_b = 0.0031\omega - 0.1482$$

where ω is the stirrer speed in rpm and τ_b is the bed shear stress in Pa. The flow-induced bed shear stress was also estimated from the pressure change in the near-bed region (i.e., in the boundary layer) measured with Preston static tube; the details of this measurement using the same annular column is explained in Geremew and Yanful (2011). The results of the measurement using these two methods were very comparable, with a maximum difference of less than 10% (Fig. 5).

Consolidation of the tailings samples

For some of the re-constituted tailings samples, the total pore-water pressure was measured during the 3 days of consolidation in the annular column. Figure 6 shows the measured total pore-water pressure of the re-constituted tailings samples: sample 13 (re-constituted Mattabi tailings), sample 14 (re-constituted Shebandowan west cell tailings), and sample 16 (re-constituted Mattabi tailings – kaolinite mixture). For sample 14, which had a fines content of 72.87%, the total pore-water pressure was much higher at the beginning of consolidation and the excess pore-water pressure started dissipating over time. This suggests that the re-constituted sample 14 shows cohesive behavior. With similar arguments, samples 13 and 16 show cohesive behavior.

Concentration of re-suspended tailings

As explained in the sample preparation section, the re-constituted Mattabi tailings were consolidated for 3 days

Fig. 4. X-ray powder pattern of Shebandowan West cell tailings.

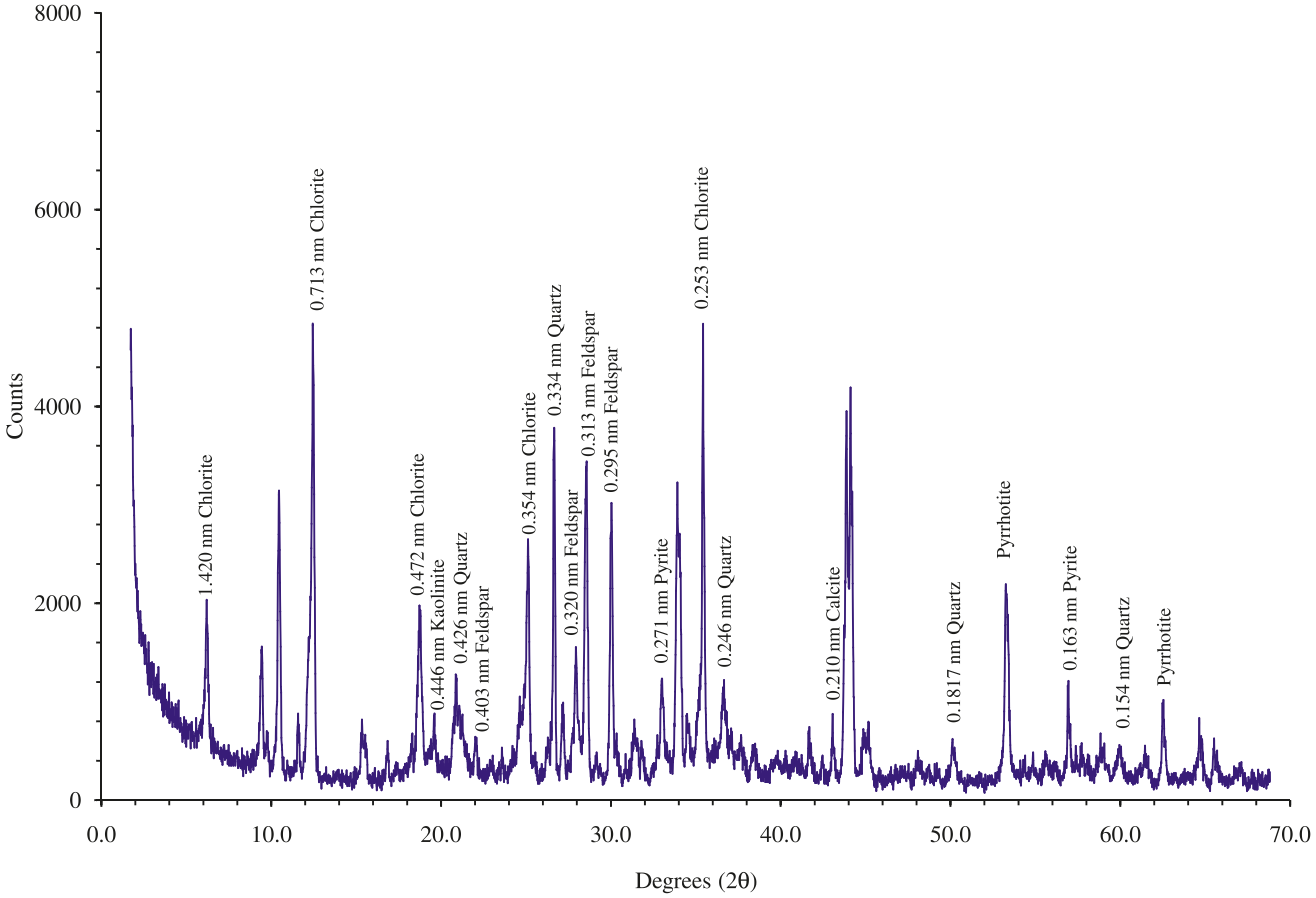

Fig. 5. LDV and Preston tube results at the mid-point of the annular flume. R^2, determination coefficient.

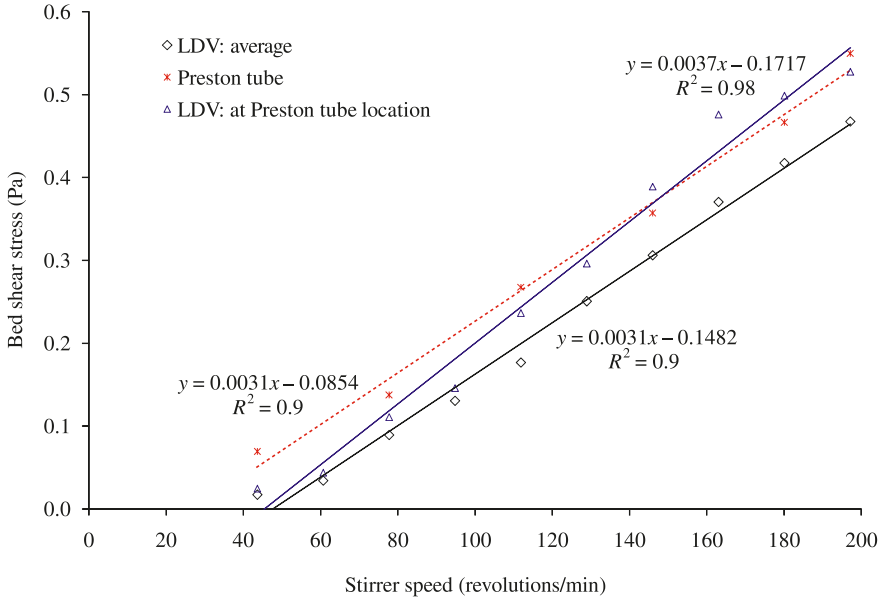

and the erosion experiments were carried out. As a means of determining the concentration of re-suspended solids, samples were taken after 10, 20, 30, and 40 min from the beginning of each shear stress increment using the sampling ports. The results of these measurements are shown in Figs. 7*a* and 7*b*. These figures also show that the erosion rate was high at the start and nearly nil at the end of each stress increment.

Critical bed shear stress for erosion and erosion rate — experimental

To formulate the erosion rate equations, the critical shear

Fig. 6. Total pore-water pressure at mid-depth of the deposited re-constituted tailings samples.

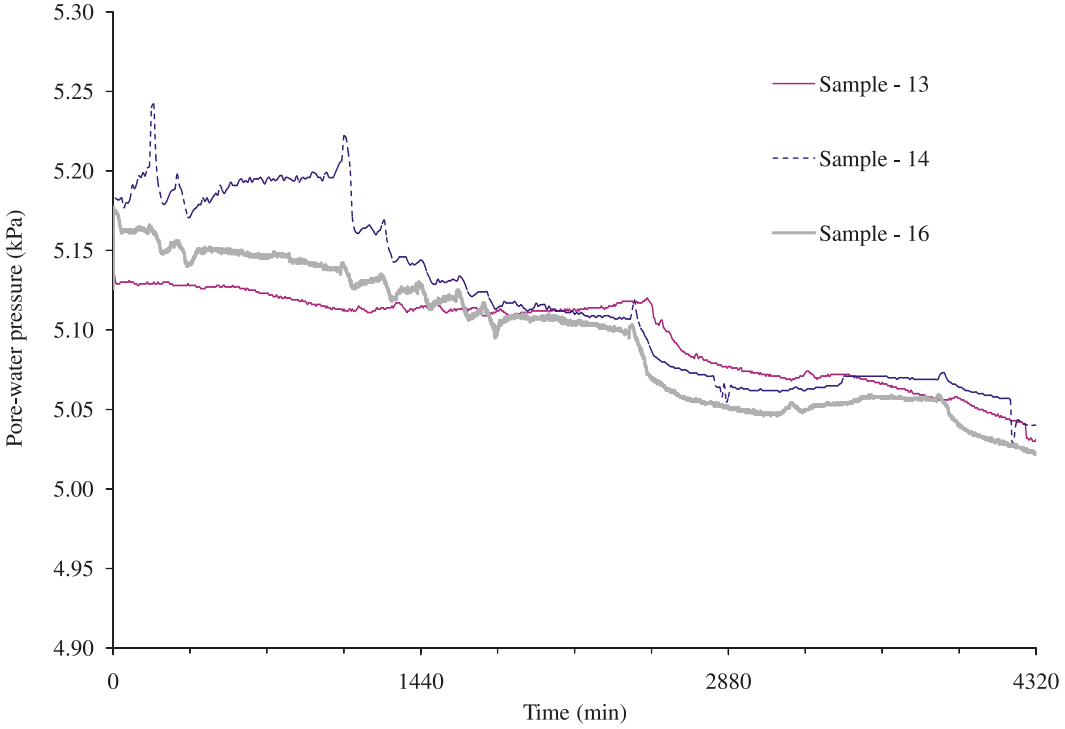

stress and the relationship between erosion rate and bed shear stress should be known. The critical shear stress has been defined by some researchers as the stress at which initiation of motion first occurs (for example, Young and Southard 1978); a second group of researchers defined it as the stress at which significant erosion first occurs (Gust and Morris 1989; Maa et al. 1998; Roberts et al. 1998); a third group defined it as the shear stress that gives zero erosion rate, which is usually done by extrapolating the erosion rate – bed shear stress curve (Partheniades 1965; Sanford and Halka 1993; Ravens and Gschwend 1999); and a fourth group defined it as an increasing critical shear stress with depth (Parchure and Mehta 1985; Kuijper et al. 1989; Amos et al. 1997). There is also no unique definition of the erosion rate. Some researchers defined it as the initial erosion rate just after the introduction of a new shear stress (Maa et al. 1998), others defined it as the erosion rate after some initial response period (Ravens and Gschwend 1999); and another group defined it as the average erosion rate during a given stress increment.

In the present study, the initial erosion rate for each shear stress increment was determined from the re-suspended tailings concentration – time relationship. The initial erosion rate was defined as the time rate of change in concentration of suspended tailings within the first 10 min of the stress increment and can be determined from eq. [2]

$$[2] \qquad E = \frac{H}{60\,000}\left(\frac{C_{10} - C_0}{t_{10} - t_0}\right)$$

where E is the erosion rate in kg·m^{-2}·s^{-1}, H (= 0.50 m) is the height of water above the tailings surface in the laboratory column in m, C_{10} and C_0 are the concentrations of re-suspended tailings particles at the beginning and end of each time step in mg·L^{-1}, and $t_{10} - t_0$ (= 10 min) is the time step in min.

The calculated initial erosion rates for the samples were plotted against the respective measured bed shear stresses and the best-fit lines were determined. The X-intercept for each of these lines at zero erosion rates represents an extrapolated value that has been taken as the critical shear stresses for the corresponding samples (Fig. 8). It should be noted that negligible rates of erosion may occur for shear stresses less than the estimated critical shear stress (Hunt and Mehta 1985). The critical shear stresses for surface erosion (τ_{cr}) of the tailings were also estimated by visually observing and examining the applied shear stress that actually created "pitting of the surface" and made "the water cloudy." The visual observations and examinations were done during the erosion experiment by noting the stirrer speed during incipient motion of the particles and estimating the corresponding shear stress. The shear stress of the bed was correlated to the stirrer speed as presented in eq. [1]. The critical shear stress for erosion (τ_{cr}) for the re-constituted mine tailing samples and other tailings are as presented in Table 4.

For all the re-constituted tailings, the results show that the critical shear stress determined from the relationship between the bed shear stress and concentrations of re-suspended solids was larger than the one determined by visual examination. This is due to the fact that at the time of initiation of motion of re-suspended particles, the concentration is so low that it is difficult to get representative samples with the sampling technique that was employed in this study.

The critical bed shear stress for erosion of the re-constituted Shebandowan tailings (sample 14) from the erosion experiment was quite low compared with the re-constituted Mattabi tailings (say, samples 12 and 13) even though its

Fig. 7. (*a*) Time–concentration and bed shear stress curves for the re-constituted tailing samples 1–8. (*b*) Time–concentration and bed shear stress curves for the re-constituted tailing samples 9–16.

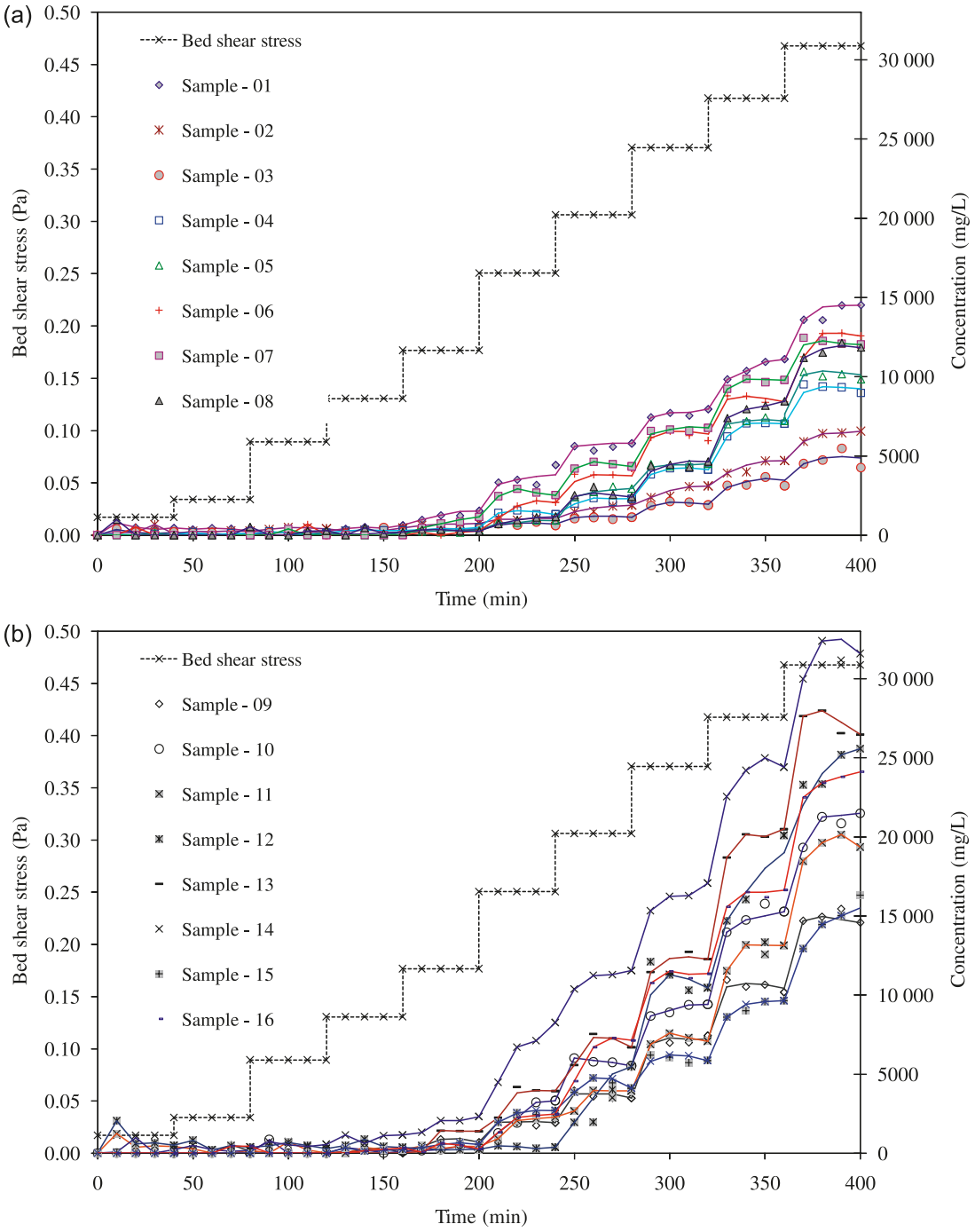

salinity was quite high (2.092 g/L) (Table 2). One of the probable reasons for this could be oxidation of the top thin layer of the 3 day consolidated re-constituted Shebandowan tailings. The transformation of sulphide minerals to secondary minerals (e.g., iron oxy hydroxides) due to oxidation can result in lower critical shear stress (Yanful et al. 1999).

Based on linear regression analysis (Fig. 9 and Table 4), a power law relationship can be used to describe the relation between the measured nondimensional excess bed shear stress, $(\tau_b - \tau_{cr})/\tau_{cr}$ (where τ_b is the bed shear stress), and the erosion rate, E. The derived relation is as shown in eq. [3] and the details of the erosion constants, α and β, are as shown in Table 4 (Fig. 9).

$$[3] \qquad E = \alpha\left(\frac{\tau_b - \tau_{cr}}{\tau_{cr}}\right)^{\beta}$$

Fig. 8. Critical shear stress estimation for the re-constituted tailings sample.

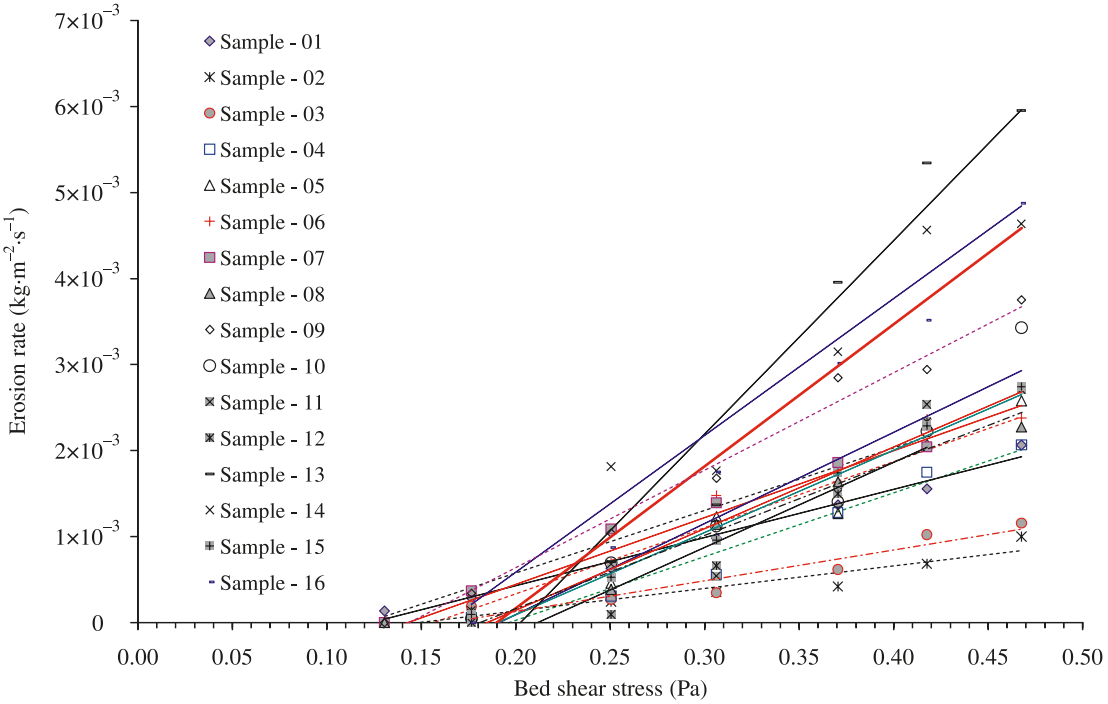

Table 4. Regression analysis of critical shear stresses and erosion rates from different tests.

Tailings name	Consolidation time (days)	Critical shear stress, τ_{cr} (Pa)	Erosion rate coefficients α	Erosion rate coefficients β	Regression coefficient, R^2	Remark
Sample - 01	3	0.034–0.123	0.0007800	0.694858	0.63	Present study
Sample - 02	3	0.090–0.147	0.0003910	0.769983	0.69	Present study
Sample - 03	3	0.130–0.168	0.0005130	1.249895	0.50	Present study
Sample - 04	3	0.177–0.196	0.0013960	1.252164	0.75	Present study
Sample - 05	3	0.177–0.181	0.0014830	1.147236	o.63	Present study
Sample - 06	3	0.130–0.143	0.0009800	1.263329	0.54	Present study
Sample - 07	3	0.090–0.120	0.0008720	1.032506	0.75	Present study
Sample - 08	3	0.130–0.157	0.0010880	1.137105	0.86	Present study
Sample - 09	3	0.130–0.144	0.0015610	1.055065	0.89	Present study
Sample - 10	3	0.180–0.191	0.0019300	0.961870	0.86	Present study
Sample - 11	3	0.130–0.190	0.0016700	1.061770	0.89	Present study
Sample - 12	3	0.180–0.211	0.0009000	1.145907	0.91	Present study
Sample - 13	3	0.18–0.202	0.000443	1.034464	0.86	Present study
Sample - 14	3	0.130–0.163	0.002538	1.121456	0.97	Present study
Sample - 15	3	0.13–0.185	0.001690	1.162950	0.98	Present study
Sample - 16	3	0.13–0.190	0.003074	1.110613	0.97	Present study
Falconbridge NTA	4	0.20–0.25	0.000040	0.830000	—	Rotating circular flume[a]
Premier Gold	4	0.09–0.10	0.000035	0.900000	—	Rotating circular flume[a]
Health Steele Upper Cell	4	0.12	0.000020	0.940000	—	Rotating circular flume[a]
Coarse tailings	—	0.21–0.25	—	—	—	Wave flume[b]
Fine tailings	—	0.20–0.22	—	—	—	Wave flume[b]

[a]Mian and Yanful 2007; Samad and Yanful 2005.
[b]Davé et al. 2003.

Table 4 shows that the linear regression coefficient R^2 is very high (0.861–0.980) for samples 8 to 16 with fines content (ϕ_{fine}) equal to or greater than 50% (Table 2), which validates the assumption of a power law relationship.

Effect of fines content on critical shear stress

The critical shear stresses for the different re-constituted tailings samples were determined experimentally. Now, as a means of examining the effect of the percentage of fines in

Fig. 9. Relationship between nondimensional excess shear stress and erosion rate.

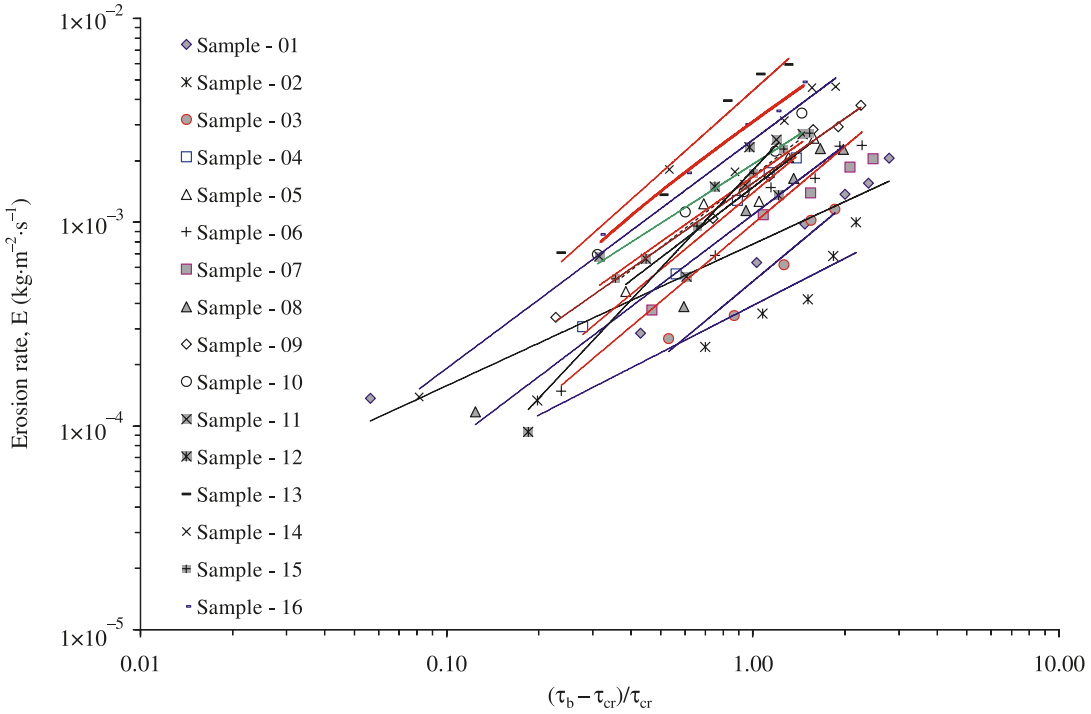

Fig. 10. Critical nondimensional shear stress versus nondimensional particle parameter.

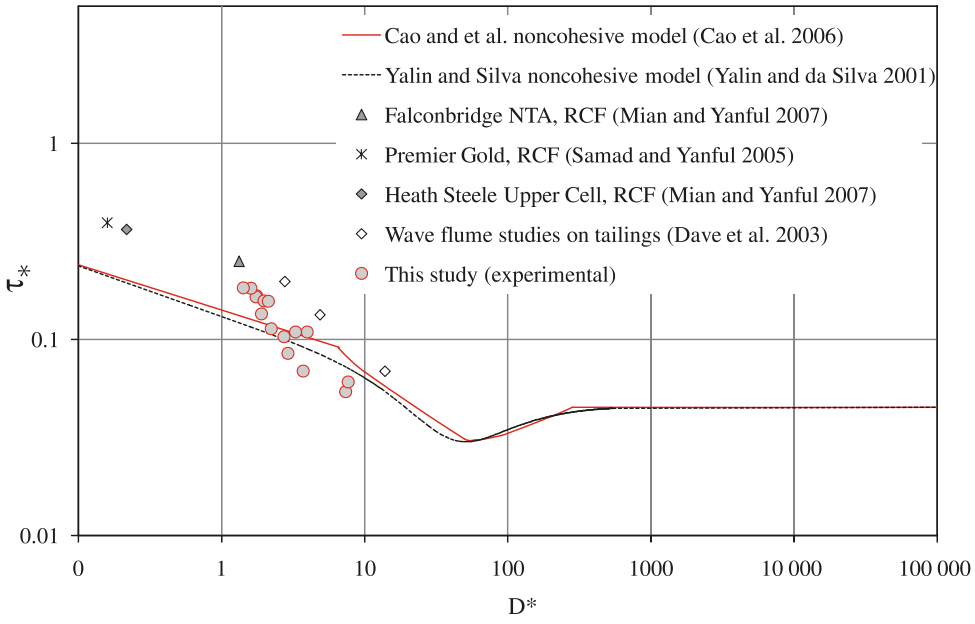

the critical shear stress, the experimentally determined nondimensional critical shear stress ($\tau_{*\text{-EX}}$) is compared to the nondimensional critical shear stress for noncohesive sediments ($\tau_{*\text{-NC}}$). Hence, the most widely used Shield's criterion for incipient motion of sediments modified by Cao et al. (2006) to give a better account of the smaller particles is used.

The Shields diagram for empirically estimating the critical shear stress of noncohesive sediments is the relation between a particle parameter (that reflects the influence of gravity, density, and viscosity) and the critical mobility (Shields') parameter. Often the empirical function of Brownlie (1981) is used to model the original Shields diagram. Most of the samples used in this study have smaller grain sizes and so it is necessary that the smaller grain sizes of the Shields diagram be adequately fitted by the model function. Cao et al. (2006) found that the original Shields diagram and Brownlie's function poorly fit the available data of the critical shear stress for sizes smaller than fine sand and they have proposed the following explicit formulation (eq. [4]) of the Shields diagram for incipient motion of sediment (Fig. 10).

Fig. 11. Difference between the nondimensional critical bed shear stress (experimentally measured) and the nondimensional critical shear stress for noncohesive sediment as a function of fines content.

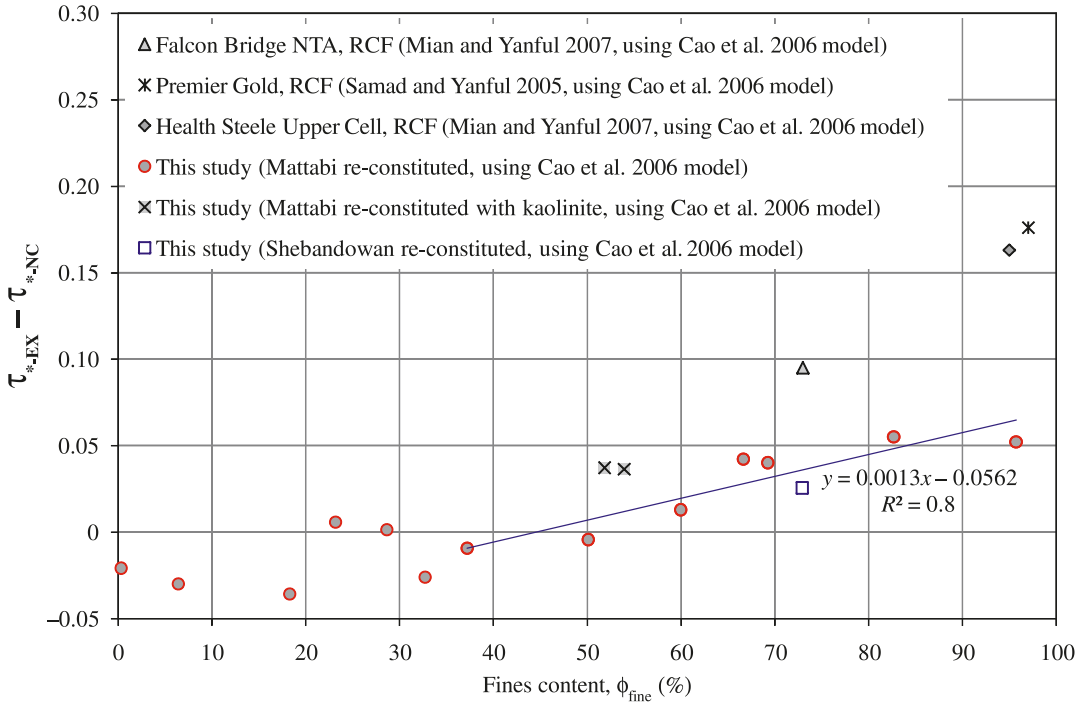

Fig. 12. Relation between the percentage of fines and the exponent of the erosion equation (β).

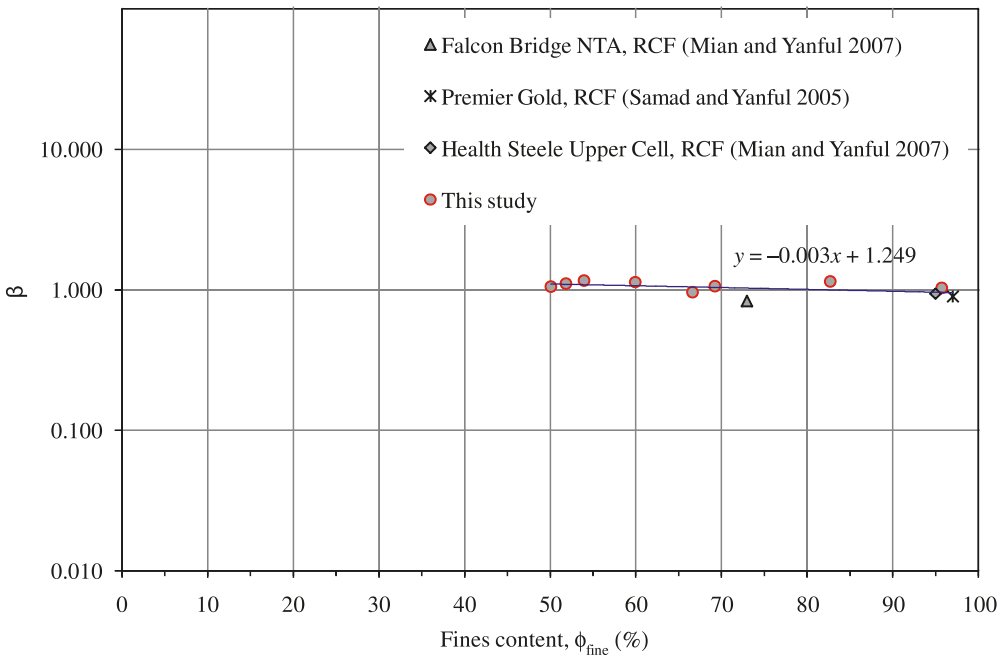

[4] $\tau_{*\text{-NC}} = 0.1414D_*^{-0.2306}$ when $D_* \leq 6.61$

$$\tau_{*\text{-NC}} = \frac{[1 + (0.0223D_*)^{2.8358}]^{0.3542}}{3.0946D_*^{0.6769}}$$

when $6.61 < D_* < 282.84$

$\tau_{*\text{-NC}} = 0.045$ when $D_* \geq 282.84$

where $\tau_{*\text{-NC}}$ is the nondimensional critical shear stress for noncohesive sediments (i.e., critical mobility parameter), D_* (= $[(s - 1)gd_*^3 / \nu^2]^{0.5}$) is the nondimensional particle parameter, s is the particle specific gravity, g is the gravitational acceleration, d_* is the characteristic grain size, and ν is the kinematic viscosity.

For a comparison, the Yalin and da Silva (2001) model has also been used. This model is described by eq. [5] and plotted in Fig. 10.

Fig. 13. Relation between the percentage of fines and coefficient of the erosion equation (α).

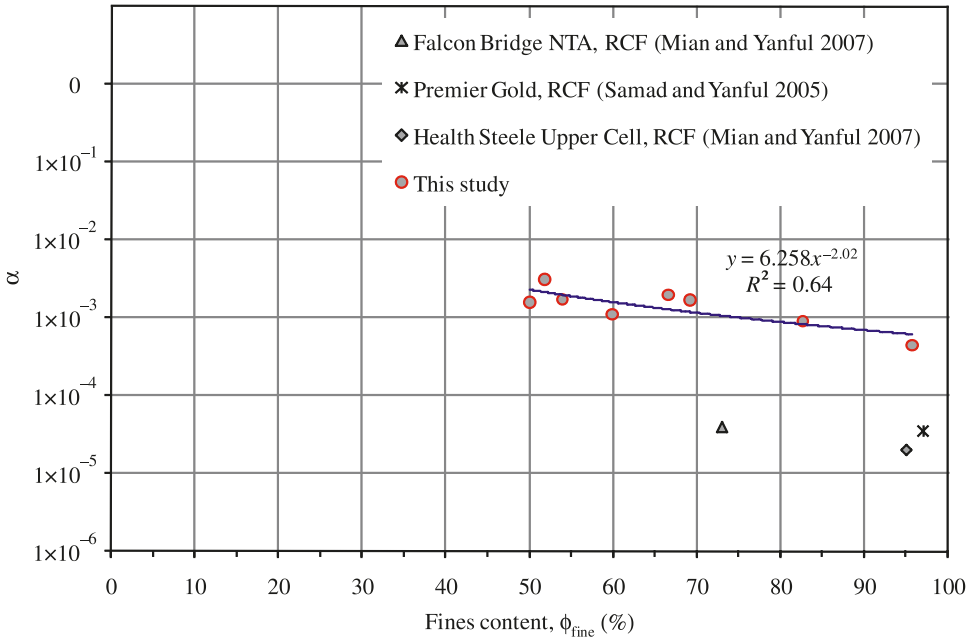

$$[5]\quad \tau_{*c\text{-}NC} = 0.13D_*^{-0.2613}\exp(-0.015D_*^{1.3333}) + 0.045[1 - \exp(-0.068D_*^{0.6667})]$$

The experimentally determined critical bed shear stress for each of the samples used in the present study has been utilized to estimate the nondimensional particle critical mobility parameter (eq. [6]). Equation [6] is adopted from the Shields' critical mobility parameter (Shields 1936)

$$[6]\quad \tau_{*\text{-}EX} = \frac{\tau_{cr}}{(\rho_s - \rho_w)gd_{50}}$$

where $\tau_{*\text{-}EX}$ is the nondimensional critical mobility parameter for the tailings of the present study, τ_{cr} is experimentally determined critical bed shear stress in Pa, ρ_s is the sediment particle density in kg/m^3, ρ_w is the density of water in kg/m^3, g is acceleration due to gravity in m/s^2, and d_{50} is the median particle size of the tailings sample in m.

Moreover, the median particle size of each of the tailings samples and their respective specific gravities were used to estimate the nondimensional particle parameters (eq. [7])

$$[7]\quad D_{*\text{-}EX} = \left[\frac{(s-1)gd_{50}^3}{\nu^2}\right]^{1/2}$$

where $D_{*\text{-}EX}$ is the nondimensional particle parameter for the tailings of the present study, s (= ρ_s/ρ) is specific gravity, and ρ is the density.

As mentioned earlier, Fig. 10 shows the criterion for incipient motion of noncohesive sediments after modification for fine sediments by Cao et al. (2006) in a log–log plot. It also shows the relationship between experimentally determined nondimensional critical bed shear stress (i.e., critical mobility parameters) and the corresponding nondimensional particle parameter for the 16 tailings samples of the present study, as well as the studies of Mian and Yanful (2007), Davé et al. (2003), and Samad and Yanful (2005). This log–log plot shows that the deviation of the nondimensional critical shear stress ($\tau_{*\text{-}EX} - \tau_{*\text{-}NC}$) of the finer samples is quite large and as the tailings particle sizes get larger, the deviation from the Cao et al. (2006) and Yalin and da Silva (2001) relations becomes smaller and smaller and, eventually, become nil.

To examine the role of fines on the cohesive behavior of the re-constituted tailings samples, the percentage of fines in each of the samples used in the present study have been plotted against the corresponding deviation of critical shear stresses ($\tau_{*\text{-}EX} - \tau_{*\text{-}NC}$) in Fig. 11. The results show that the critical bed shear stress increases rapidly when the fines content of the tailings material gets above 50% (Fig. 11). This rapid increase in erosion resistance of the tailings is from the developed cohesion resistance of the fine-sized tailings because, as Table 2 suggests, the salinity and other chemical properties of the re-constituted tailings samples do not significantly influence the critical shear stress. Therefore, for the tailings investigated in the present study, a fines content of 50% to 55% (with clay content much less than 5%) can be considered as a transition from noncohesive to cohesive tailings. In general, the results suggest that the presence of 50% to 55% fines in tailings is sufficient to make the tailings cohesive and significantly increase its resistance to surface erosion for a confined water system, such as a tailings pond. In the transition from noncohesive to cohesive behavior, the tailings can be cohesive or noncohesive depending on the prevailing boundary condition and the chemical and mineralogical characteristics of the tailings under consideration.

As shown in Fig. 11, the data with fines content higher than 50% ($\phi_{fine} > 50\%$) have been best-fitted with a linear curve resulting in eq. [8] with a coefficient of correlation of 0.84 ($R^2 = 0.84$).

$$[8]\quad \tau_{*\text{-}EX} \geq \tau_{*\text{-}NC} + 0.0013\phi_{fine} - 0.0562 \quad \text{for } \phi_{fine} > 50\%$$

$$\tau_{*\text{-}EX} = \tau_{*\text{-}NC} \quad \text{for } \phi_{fine} \leq 50\%$$

Equation [8] suggests that tailings with a fines content less than 50% can be considered noncohesive.

Erosion rate constants, α and β

As explained earlier, eq. [3] can reasonably describe the relation between the measured nondimensional excess bed shear stress and the re-suspension rate. The values of the erosion constants, α and β, have been estimated by regression analysis from the measured erosion data. As shown in Fig. 12, for $\phi_{fine} > 50\%$, the relationship between the fines content (ϕ_{fine} in percent) and β can be estimated by eq. [9].

$$[9] \qquad \beta = -0.0030\phi_{fine} + 1.2496$$

Equation [9] shows that the β value for this study varies between 1.2496 ($\phi_{fine} = 0\%$) and 0.945 ($\phi_{fine} = 100\%$) with an average value of 1.0973. This suggests that the value of β can be taken as 1 for all practical purposes for the samples and that the erosion equation will be linear (eq. [10])

$$[10] \qquad E = \alpha\left(\frac{\tau_b - \tau_{cr}}{\tau_{cr}}\right)$$

Equation [10] is similar to the Ariatheniades–Partheniades equation, which is most often used to describe the erosion of cohesive natural sediments (Partheniades 1965; Ariathurai 1974). The relationship between the percentage of fines and α is shown in Fig. 13. The results show that the value of the erosion rate constant, α, decreases with an increase in fines content. This decrease is a result of the increase in cohesiveness at a fines content of 50% or greater.

Data from the rotating circular flume (Samad and Yanful 2005; Mian and Yanful 2007) and the wave flume (Davé et al. 2003) were also analyzed and plotted as shown in Fig. 11 (Table 2). It is seen that the deviation of $\tau_{*\text{-EX}}$ from $\tau_{*\text{-NC}}$ is much higher than that of the re-constituted tailings samples of the present study. This may be due to the effect of salinity, the presence of organic matter, and other physical and chemical characteristics of the tailings.

Summary and conclusions

In the present study, the erosion characteristics of 16 laboratory re-constituted mine tailings were measured using a Plexiglas annular column under a 50 cm water cover. The annular column was 30 cm in diameter, 120 cm in height, and had a 9 cm annular flow width (Fig. 1). Re-suspension was introduced through a motor-driven Teflon stirrer to investigate the initiation of motion and subsequent re-suspension of newly deposited laboratory re-constituted mine tailings. The velocity field in the column was calibrated by LDV and the pressure change in the boundary layer was also measured by Preston tube. The following conclusions are made from the laboratory experimental results.

- The bed shear stress estimated from the near-bed velocity profile (using an LDV) was in good agreement with values measured with the Preston tube. Therefore, the bed shear stress can be estimated accurately and inexpensively with a Preston static tube alone.
- The erosion rate for the tailings was high at the start and was nearly nil towards the end of each stress increment.
- The critical shear stresses for erosion (τ_{cr}) for the tailings varied between 0.09 and 0.23 Pa for a range of fines content.
- The critical shear stress for erosion of the re-constituted Shebandowan west cell tailings was quite low compared with that of the re-constituted Mattabi tailings even though the salinity of the Shebandowan tailings was quite high (2.092 g/L). This could be due to the fact that the top thin layer of the 3 day consolidated, re-constituted Shebandowan tailings was probably oxidized.
- The linear regression analysis validates the assumption of a power law relationship between the measured nondimensional excess bed shear stress, $(\tau_b - \tau_{cr})/\tau_{cr}$, and the erosion rate, E, for the samples that showed cohesive behavior (samples 8 to 16).
- It was observed that the nondimensional critical shear stresses showed deviation from noncohesive sediments model results of Cao et al. (2006) and Yalin and da Silva (2001) at a fines content (<63 μm) greater than 50%–55%. This suggests that 50% to 55% fines in tailings (with clay content less than 5%) can be considered sufficient to make the tailings cohesive and significantly increase its resistance to surface erosion for a confined water system, such as a tailings pond.
- An empirical equation that shows the relation between the boundary shear stress deviation ($\tau_{*\text{-EX}} - \tau_{*\text{-NC}}$) and the percentage of fines in the tailings was proposed.
- Based on the regression analysis, a power law relationship can be used to describe the relation between the measured nondimensional excess bed shear stress, $(\tau_b - \tau_{cr})/\tau_{cr}$, and the re-suspension rate, E.
- It is also proposed that the value of β in the power law erosion equation, $E = \alpha[(\tau_b - \tau_{cr})/\tau_{cr}]^{\beta}$, can be taken as 1 for mine tailings that show cohesive behavior. This, indeed, is similar to Ariatheniades–Partheniades (Partheniades 1965), which is most often used in the erosion of cohesive natural sediments.

Acknowledgments

The work described in this paper was supported with funding from Inco Limited and the Natural Sciences and Engineering Research Council of Canada (NSERC) under a Collaboration Research and Development Project Grant awarded to Dr. E.K. Yanful.

References

Amos, C.L., Feeney, T., Sutherland, T.F., and Luternauer, J.L. 1997. The stability of fine-grained sediments from the Fraser River delta. Estuarine, Coastal and Shelf Science, **45**(4): 507–524. doi:10.1006/ecss.1996.0193.

Ariathurai, R. 1974. A finite element model for sediment transport in estuaries. Ph.D. dissertation, University of California, Davis, Calif.

Braja, M.D. 2002. Soil mechanics laboratory manual. Oxford University Press, New York.

Brownlie, W.R. 1981. Prediction of flow depth and sediment discharge in open-channels. W.M. Kech Laboratory. Hydraulics and Water Resources, California Institute of Technology, Pasadena, Calif.

Cao, Z., Pender, G., and Meng, J. 2006. Explicit formulation of the Shields diagram for incipient motion of sediment. Journal of Hydraulic Engineering, **132**(10): 1097–1099. doi:10.1061/(ASCE)0733-9429(2006)132:10(1097).

Davé, N.K., Krishnappan, B.G., Davies, M., Reid, I., and Lanteigne, L. 2003. Erosion characteristics of underwater deposited mine

tailings. Mining and the Environment, Canada Natural Resources, Sudbury, Ont.

Geremew, A.M., and Yanful, E.K. 2011. Behavior of mine tailings under cyclic hydraulic loading. Canadian Journal of Civil Engineering, **38**(2): 131–140. doi:10.1139/L10-121.

Gust, G., and Morris, M.J. 1989. Erosion thresholds and entrainment rates of undisturbed in situ sediments. Journal of Coastal Research, **S5**: 87–100.

Hunt, S.D., and Mehta, A.J. 1985. An evaluation of laboratory data on erosion of fine sediment beds. *In* Particulate and multiphase processes: Colloidal and interfacial phenomena. Hemisphere, Washington, D.C. Vol. 3, pp. 503–518.

Kuijper, C., Cornelisse, J.M., and Winterwerp, J.C. 1989. Research on erosive properties of cohesive sediments. Journal of Geophysics Research, **94**(C10): 14341–14350.

Maa, J.P.-Y., Sanfort, L.P., and Halka, J.P. 1998. Sediment resuspension characteristics in Baltimore Harbor, Maryland. Marine Geology, **146**(1–4): 137–145. doi:10.1016/S0025-3227(97)00120-5.

McCave, I.N., Manighetti, B., and Robinson, S.G. 1995. Sortable silt and fine sediment size/composition slicing: parameters for palaeocurrent speed and palaeoceanography. Paleoceanography, **10**(3): 593–610. doi:10.1029/94PA03039.

Mian, H.M., and Yanful, E.K. 2007. Erosion characteristics and resuspension of subaqueous mine tailings. Journal of Environmental Engineering and Science, **6**(2): 175–190. doi:10.1139/S06-040.

Mignoit, C. 1981. Estuarine sediment dynamics - cohesive and non-cohesive materials. Defence Research Information Center, **6**(4): 359–432.

Mitchell, J.K., and Soga, K. 1997. Fundamentals of soil behavior. 3rd ed. John Wiley & Sons, Inc., New York.

Mitchener, H., and Torfs, H. 1996. Erosion of mud/sand mixtures. Coastal Engineering, **29**(1–2): 1–25. doi:10.1016/S0378-3839(96)00002-6.

Parchure, M.T., and Mehta, A.J. 1985. Erosion of soft cohesive sediment deposits. Journal of Hydraulic Engineering, **111**(10): 1308–1326. doi:10.1061/(ASCE)0733-9429(1985)111:10(1308).

Partheniades, E. 1965. Erosion and deposition of cohesive soils. Journal of the Hydraulic Division, ASCE, **91**(1): 105–139.

Partheniades, E. 2006. Engineering properties and hydraulic behavior of cohesive sediments. CRC Press, Taylor and Francis Group, New York.

Paterson, D.M. 1997. Biological mediation of sediment erodibility: ecology and physical dynamics. *In* Cohesive sediments. *Edited by* N. Burt, R. Parker, and J. Watts. Wiley and Sons Ltd., New York. pp. 215–229.

Paterson, D.M., and Daborn, G.R. 1991. Sediment stabilization by biological action: significance for coastal engineering. *In* Developments in coastal engineering. *Edited by* D.H. Peregrine and J.H. Loveless. University of Bristol, Bristol, UK. pp. 111–119.

Peacey, V., and Yanful, E.K. 2003. Metal mine tailings and sludge codeposition in a tailings pond. Water, Air, and Soil Pollution, **145**(1): 307–339. doi:10.1023/A:1023624827766.

Raudkivi, A.J. 1998. Loose boundary hydraulics. A.A. Balkema, Rotterdam, the Netherlands.

Ravens, T.M., and Gschwend, P.M. 1999. Flume measurements of sediment erodability in Boston Harbor. Journal of Hydraulic Engineering, **125**(10): 998–1005. doi:10.1061/(ASCE)0733-9429(1999)125:10(998).

Roberts, J., Jepsen, R., Gotthard, D., and Lick, W. 1998. Effects of particles size and bulk density on erosion of quartz particles. Journal of Hydraulic Engineering, **124**(12): 1261–1268. doi:10.1061/(ASCE)0733-9429(1998)124:12(1261).

Samad, M.A., and Yanful, E.K. 2005. A design approach for selecting the optimum water cover depth for subaqueous disposal of sulfide mine tailings. Canadian Geotechnical Journal, **42**(1): 207–228. doi:10.1139/t04-094.

Sanford, L.P., and Halka, J.P. 1993. Assessing the paradigm of mutually exclusive erosion and deposition of mud, with examples from upper Chesapeake Bay. Marine Geology, **114**(1–2): 37–57. doi:10.1016/0025-3227(93)90038-W.

Shields, A. 1936. Application of similarity principles and turbulence research to bed-load movement. Mitteilunger der Preussischen Versuchsanstalt für Wasserbau und Schiffbau, **26**: 5–24.

Soulsby, R. 1997. Dynamics of marine sands. A manual for practical applications. Thomas Telford Publishing, London.

Van Ledden, M., van Kesteren, W.G.M., and Winterwerp, J.C. 2004. A conceptual framework for the erosion behavior of sand–mud mixtures. Continental Shelf Research, **24**(1): 1–11. doi:10.1016/j.csr.2003.09.002.

Whitehouse, R., Soulsby, R., Roberts, W., and Mitchener, H. 2000. Dynamics of estuarine muds. A manual for practical applications. Thomas Telford Publishing, London.

Winterwerp, J.C., Cornelisse, J.M., and Kuijper, C. 1990. Parameters to characterize natural muds. *In* Abstract Volume, International Workshop on Cohesive Sediments, Brussels, Belgium. Royal Belgian Institute of Natural Sicence. pp. 103–105.

Yalin, M.S., and da Silva, A.M.F. 2001. Fluvial processes. IAHR Monograph. International Association of Hydro-Environment Engineering and Research (IAHR), Delft, the Netherlands.

Yanful, E.K., and Catalan, L.J.J. 2002. Predicted and field-measured resuspension of flooded mine tailings. Journal of Environmental Engineering, **128**(4): 341–351. doi:10.1061/(ASCE)0733-9372(2002)128:4(341).

Yanful, E.K., and Verma, A. 1999. Oxidation of flooded mine tailings due to resuspension. Canadian Geotechnical Journal, **36**(5): 826–845. doi:10.1139/cgj-36-5-826.

Yanful, E.K., Simms, P.H., and Payant, S.C. 1999. Soil cover for controlling acid generation in mine tailings: a laboratory evaluation of the physics and geochemistry. Water, Air, and Soil Pollution, **114**(3/4): 347–375. doi:10.1023/A:1005187613503.

Yanful, K.E., Verma, A., and Straatman, A.S. 2000. Turbulence driven metal release from suspended pyrrhotite tailings. Journal of Geotechnical and Geoenvironmental Engineering, **126**(12): 1157–1165. doi:10.1061/(ASCE)1090-0241(2000)126:12(1157).

Young, R.A., and Southard, J.B. 1978. Erosion of fine-grained marine sediment: Sea-floor and laboratory experiments. Geological Society of America Bulletin, **89**(5): 663–672. doi:10.1130/0016-7606(1978)89<663:EOFMSS>2.0.CO;2.